

Supplemental Figures

Figure S1

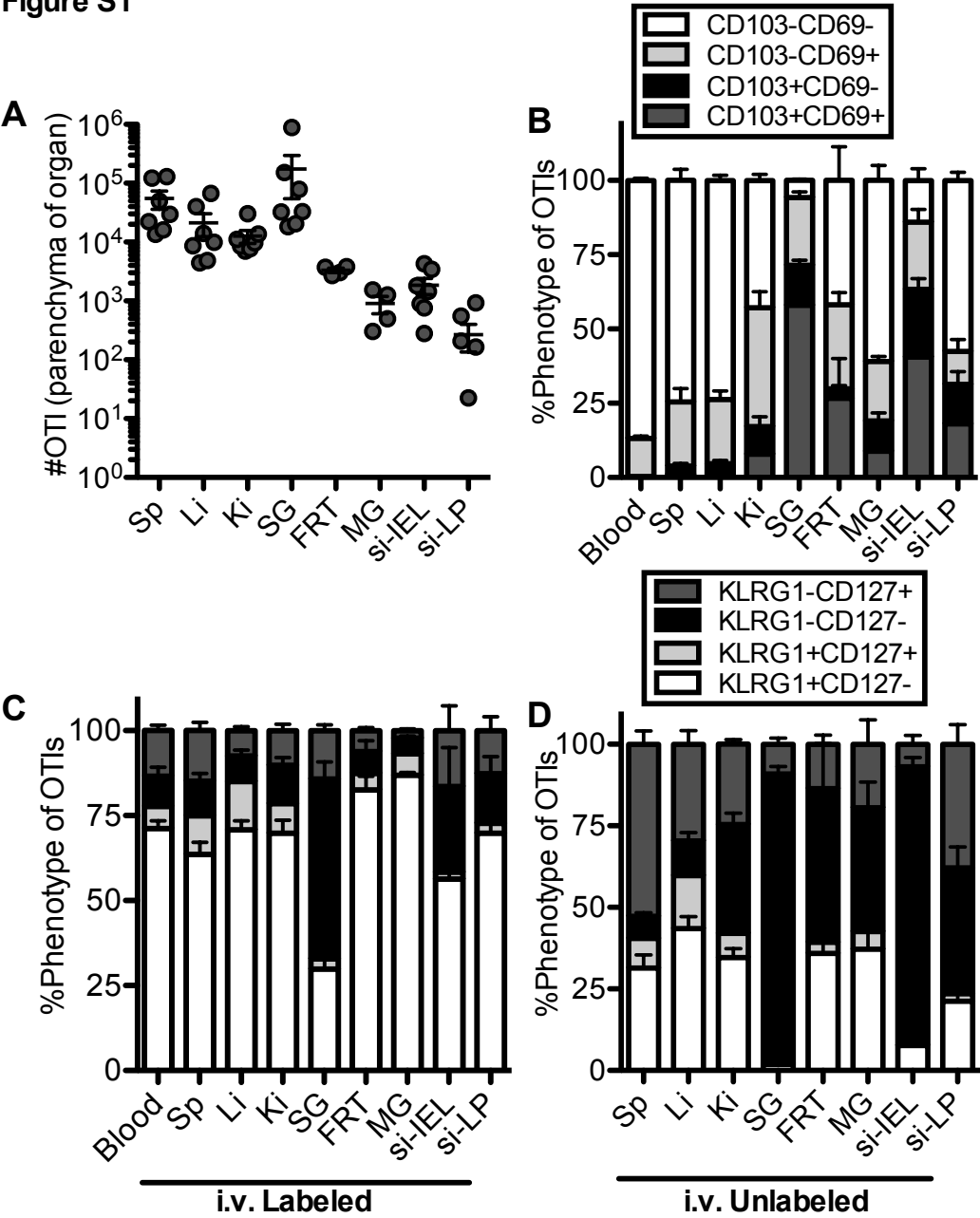


Figure S1 (Related to Figure 1): OT-Is in the parenchyma of organs display T_{RM} phenotype rather than an effector phenotype. (A) Absolute numbers of OT-Is from Figure 1 protected from i.v. staining within each organ. (B) OTIs in the unlabeled fraction of each organ were analyzed for expression of CD103 and CD69. Shown is the frequency of the indicated phenotype among OT-Is. (C, D) OT-Is that were either labeled or unlabeled with i.v. injected anti-CD8 α antibody were analyzed for expression of KLRG-1 and IL-7R α (CD127). Frequency of the indicated phenotype among OT-Is within the i.v. labeled (C) or unlabeled (D) fraction of each organ. Results are a combination of two independent experiments (n=4-7). Error bars represent the standard error of the mean.

Figure S2

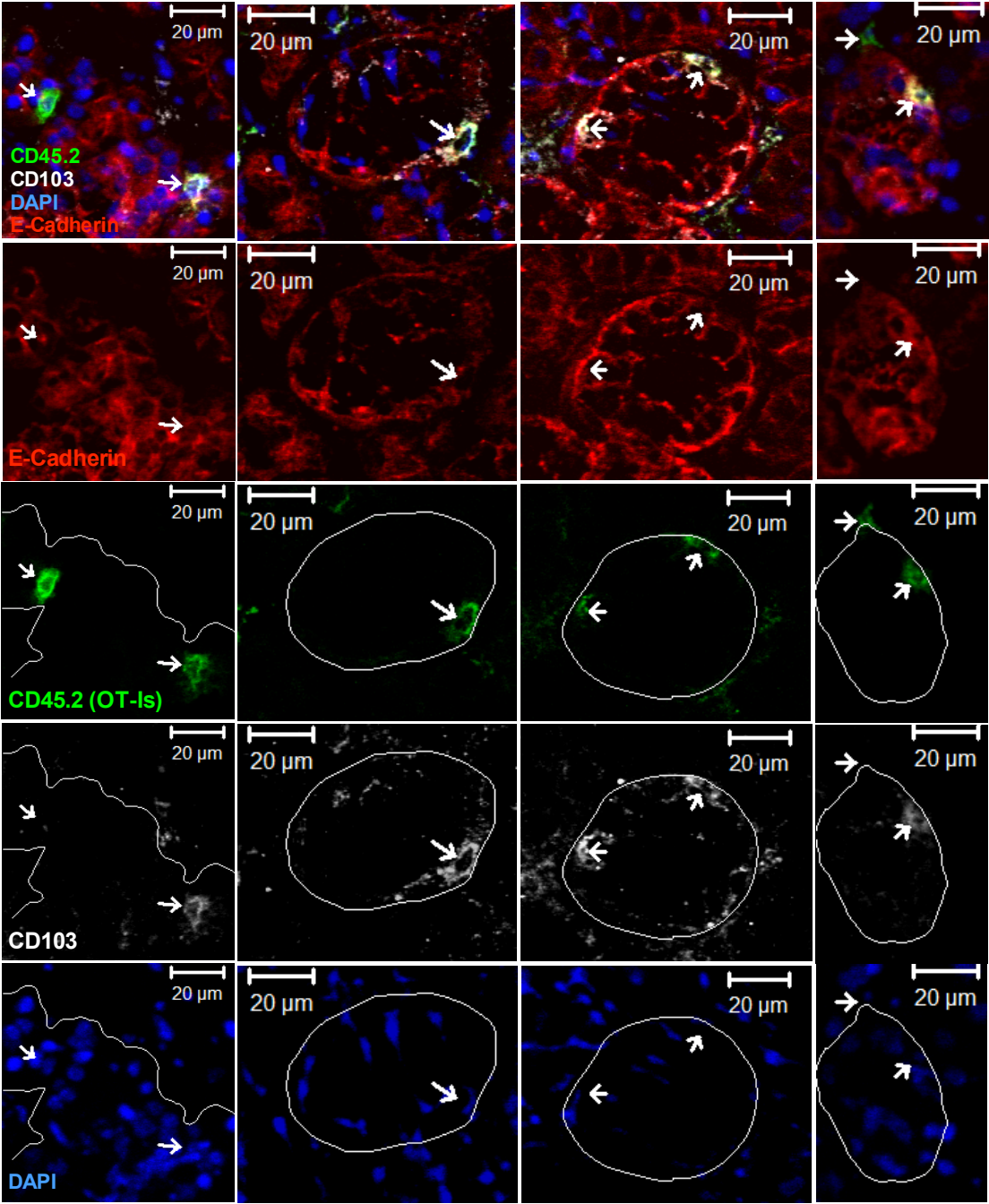


Figure S2 (Related to Figure 1): MCMV specific cells adopt an intraepithelial localization salivary gland. Shown are OT-Is (identified by CD45.2 expression, shown in green and marked by arrows) with and without CD103 expression (shown in white) as determined by immunofluorescent staining of the salivary gland >12 weeks after adoptive transfer and infection. OT-Is were frequently embedded in the epithelium (identified by E-cadherin, shown in red) in structures that are consistent with acinii and ducts. OT-Is that were not intraepithelial were frequently in close contact with epithelial structures. Overlays in bottom three rows mark the boundaries of epithelial structures. DAPI staining of the nucleus is shown in blue. Data is representative of four mice.

Figure S3

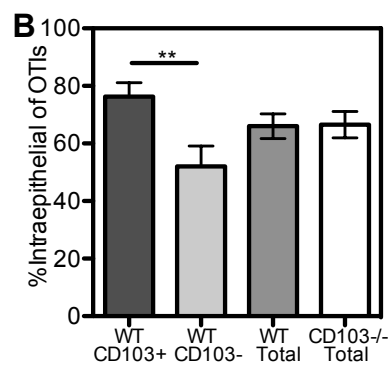
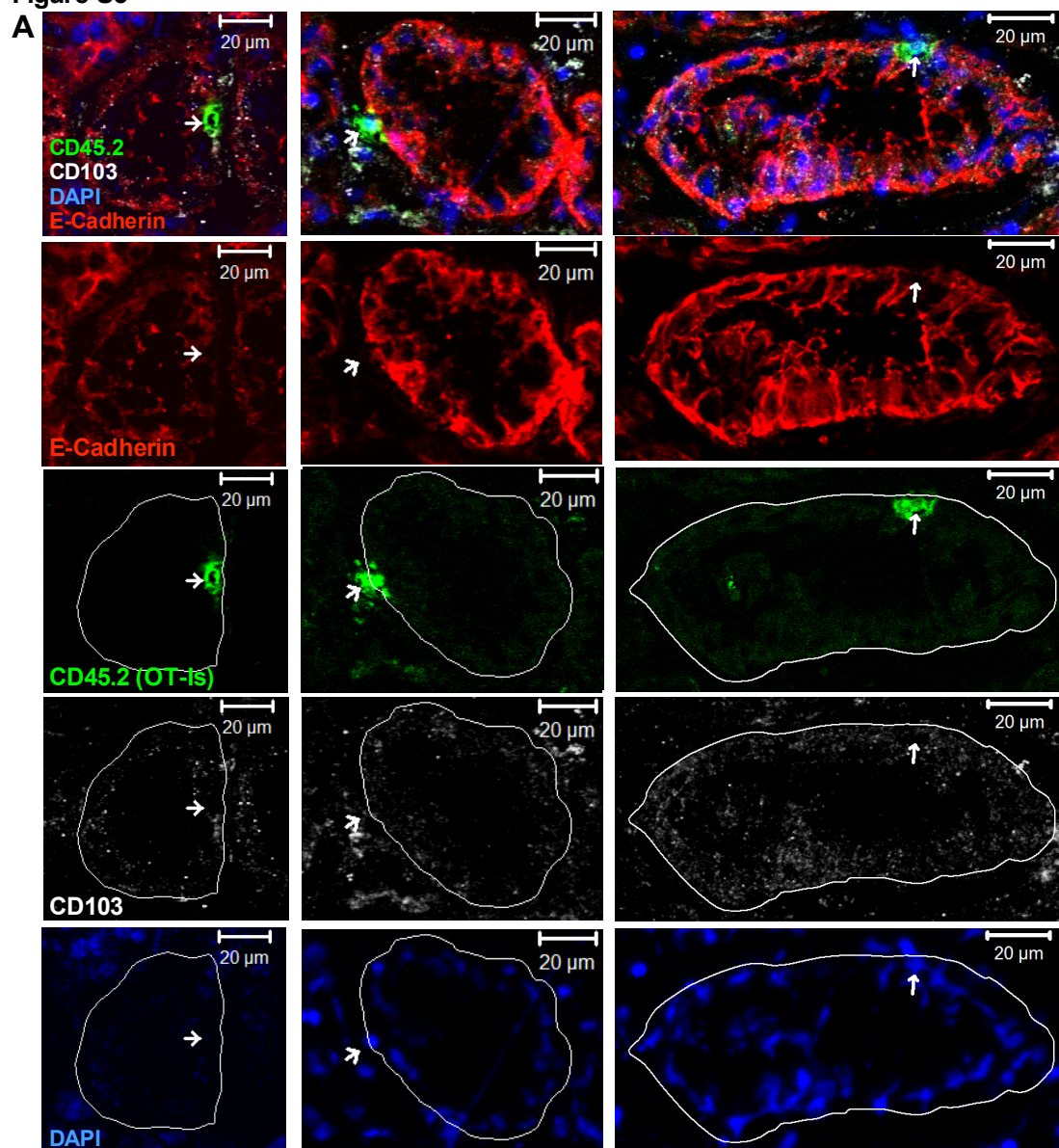


Figure S3 (Related to Figure 2): CD103 expression is not required for intraepithelial localization of MCMV-specific CD8s in the salivary gland. As described in Figure 2, wild type or CD103^{-/-} OT-Is were adoptively transferred and challenged by MCMV-OVA. (A) The localization of OT-Is in the salivary gland was examined by immunofluorescent staining >12 weeks post infection. CD103^{-/-} OT-Is (identified by CD45.2 expression, shown in green and marked with arrows) have a distribution similar to wild type OT-Is and are readily found embedded in the epithelium (identified by E-cadherin, shown in red). CD103 staining is shown in white and DAPI staining of the nucleus is shown in blue. Overlays in bottom three rows mark the boundaries of epithelial structures. Data are representative of three mice. (B) Shown is the percent of OT-Is that were embedded within the epithelium for wild type OT-Is with or without expression of CD103 and total wild type OT-Is compared to total CD103^{-/-} OT-Is. Intraepithelial cells were defined as cells that were fully surrounded by E-cadherin-expressing cells. Data are representative of 3 mice with CD103^{-/-} OT-Is and 4 mice with wild-type OT-Is. Statistical significance was measured by paired student's t-tests (*p<.05, **p<.01, ***p<.001).

Figure S4

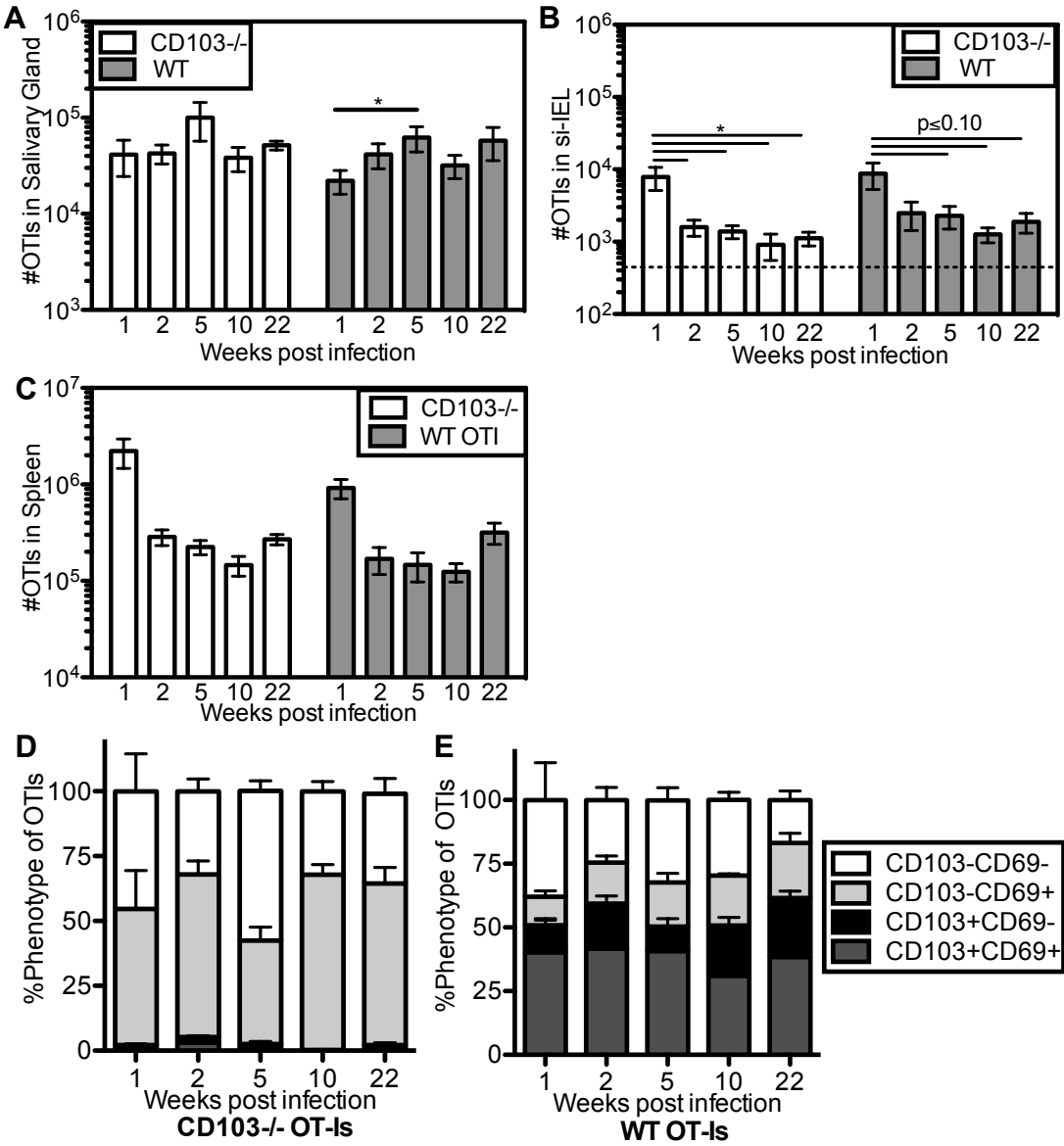


Figure S4 (Related to Figure 2): Maintenance and phenotype of wild-type and CD103^{-/-} OT-IIs in the spleen and small intestine IEL fraction. As in Figure 2, wild type and CD103^{-/-} OT-IIs were mixed together in the same mice, challenged with MCMV-OVA and cohorts were sacrificed at different times post infection. Absolute numbers of WT and CD103^{-/-} OT-IIs in the salivary gland (A) small intestine IEL (B) and spleen (C) over time. Dotted line in B indicates the limit of detection. (D, E) Frequency of the indicated phenotype within CD103^{-/-} OT-IIs (D) and WT OT-IIs (E) in the small intestine IEL over time. Results are combined from two independent experiments (n=7). Error bars represent the standard error of the mean. Statistical significance was measured by paired student's t-tests (*p<.05, **p<.01, ***p<.001).

Figure S5

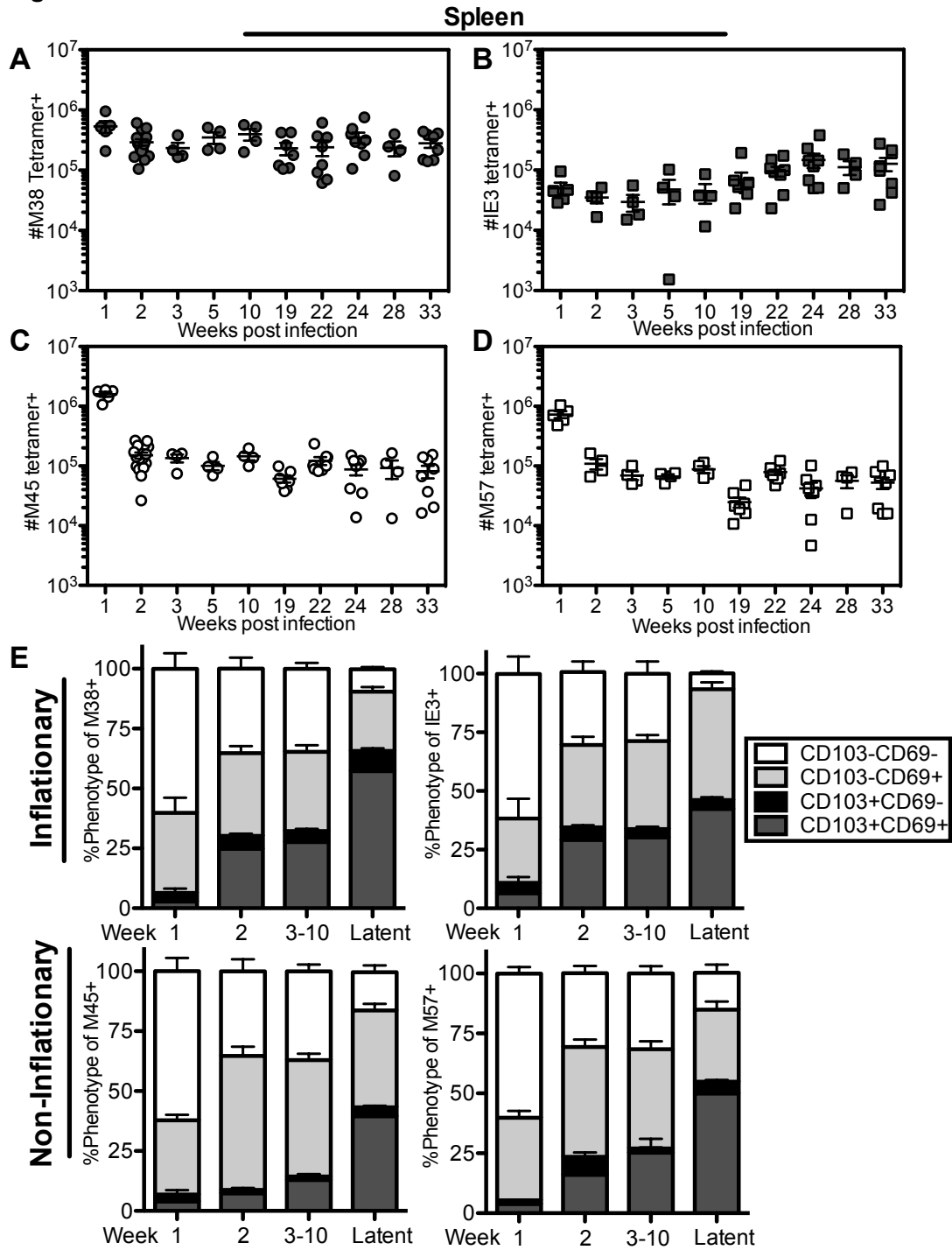


Figure S5 (Related to Figure 3): Inflationary CD8s are preferentially maintained in the salivary gland during the latent stages of infection. Absolute numbers of CD8s in the spleen specific for inflationary epitopes M38(A) and IE3 (B) and non-inflationary epitopes M45 (C) and M57 (D). Data are from the same animals described in Figure 3. (E) Frequency of the indicated phenotype among antigen specific CD8s at different times post infection. Data is combined from 7 independent experiments (n=4-16 per time point).

Figure S6

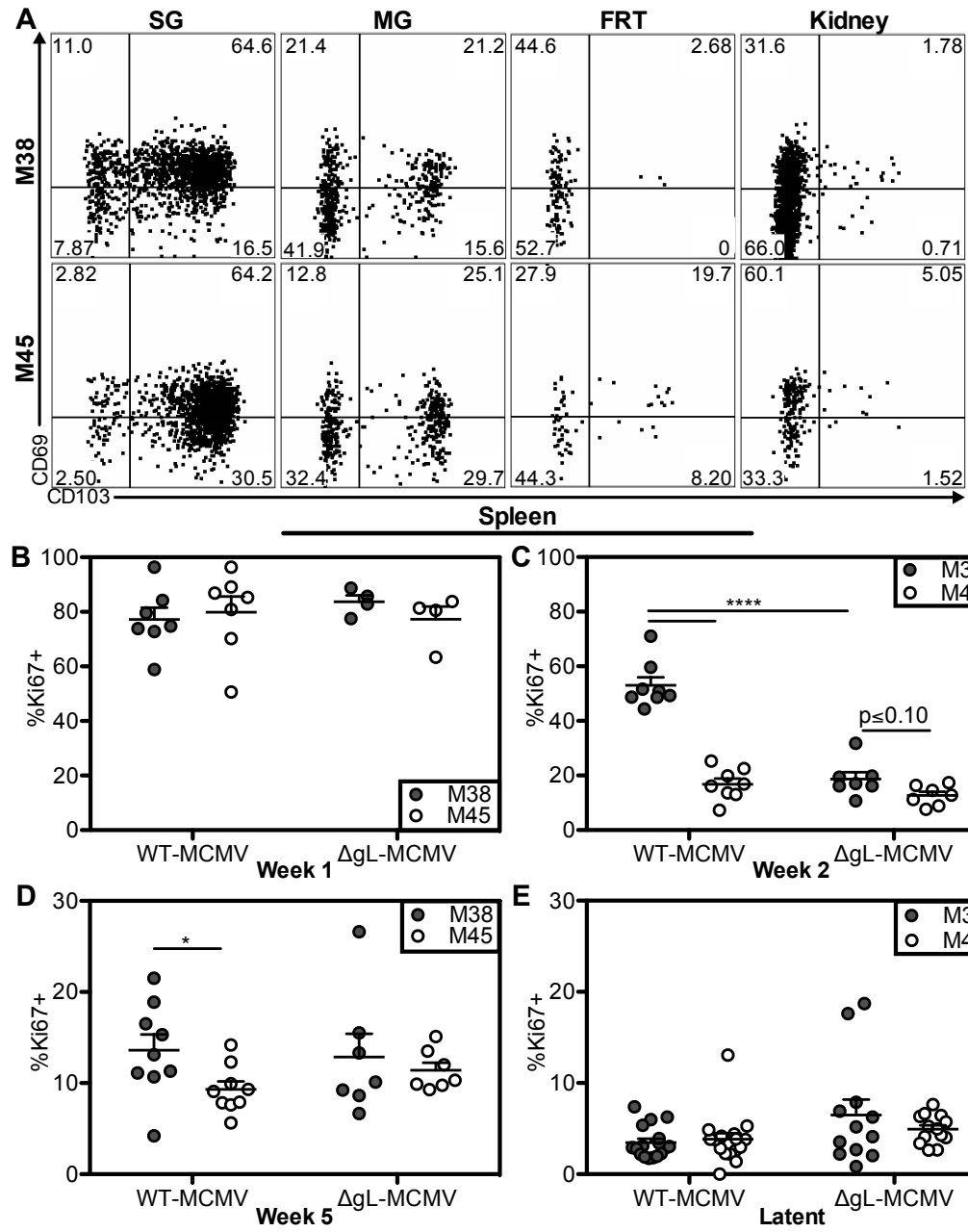


Figure S6 (Related to Figure 4): Viral replication in the salivary gland does not drive formation or replication of MCMV specific T_{RM} in the salivary gland. Mice were infected with spread defective Δ gL-MCMV and sacrificed >12 weeks post infection. Shown are representative FACS plots of CD103 and CD69 expression on M38-specific (top) and M45-specific (bottom) CD8s in the salivary gland, mammary gland, female reproductive tract and kidney. Frequency of Ki67 expression among antigen specific CD8s in the spleen at day 7 (B) day 14 (C) day 35 (D) or at latent times (E) post infection with wild type MCMV or Δ gL-MCMV. Error bars represent the standard error of the mean.

Figure S7

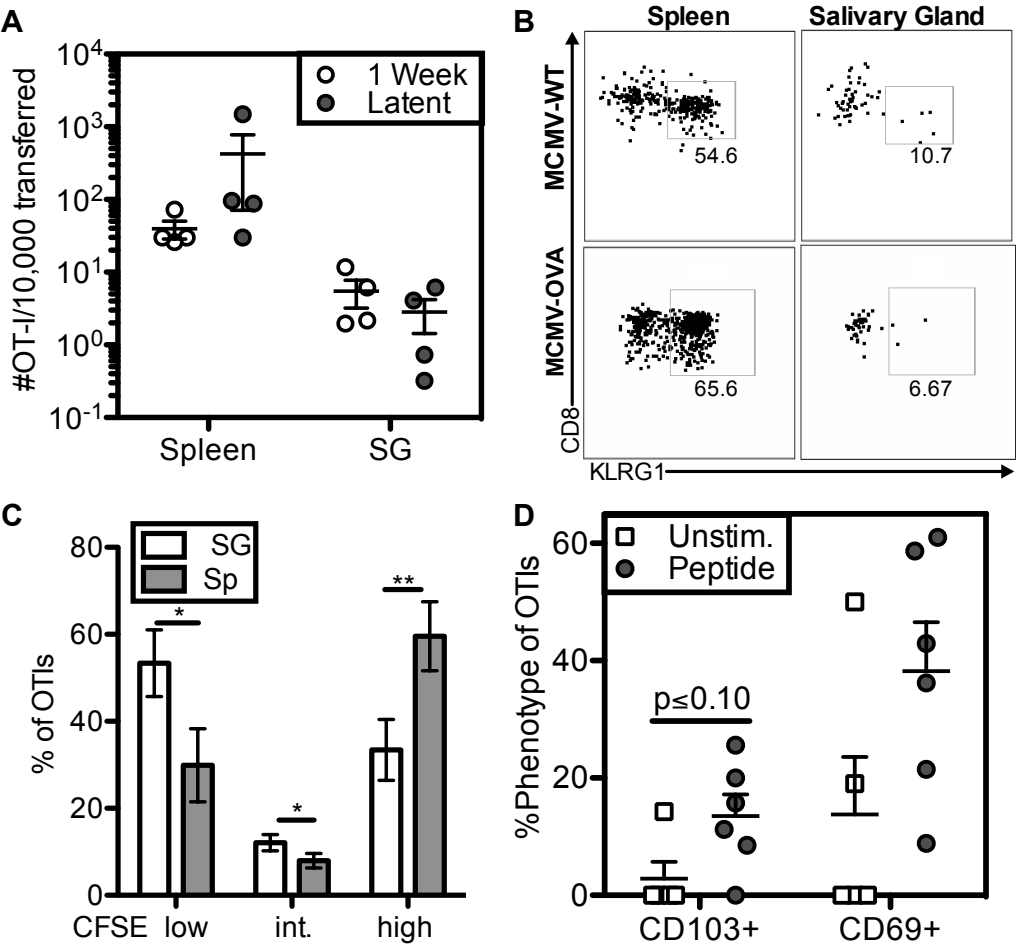


Figure S7 (Related to Figure 7): Inflationary CD8s can become T_{RM} in the salivary gland during latent infection. OT-Is were isolated from the spleens of mice at either 1 week or >12 weeks after MCMV-OVA infection and transferred into congenic naive mice. (A) Number of OT-Is in the indicated organ of naive recipients per 10,000 transferred OT-Is. (B) Representative FACS plots of KLRG1 expression on transferred OT-Is in the spleen and salivary gland 2-4 weeks after transfer into MCMV-WT or MCMV-OVA latently infected mice. (C) Frequency of donor OT-Is expressing high (undiluted CFSE intensity), low (fully diluted CFSE) and intermediate levels of CFSE in the spleen and salivary gland of MCMV-OVA latently infected recipients. (D) Frequency of CD103 and CD69 expression on OT-Is after in vitro stimulation and transfer into naive recipients. Error bars represent the standard error of the mean. Statistical significance was measured by unpaired student's t-tests (*p<.05, **p<.01, ***p<.001).

Supplemental Materials

Primers for QPCR were taken from the following: Gapdh and TGF β 1(Stock et al., 2014), TNF α (Fontenot et al., 2003), and IL-33 (Li et al., 2014).

Primer	Sequence
Gapdh Forward	CCA GGT TGT CTC CTG CGA CTT
Gapdh Reverse	CCT GTT GCT GTA GCC GTA TTC A
TGF β 1 forward	ACC ATG CCA ACT TCT GTC TG
TGF β 1 reverse	CGG GTT GTG TTG GTT GTA GA
TNF α forward	ACT GAA CTT CGG GGT GAT CG
TNF α reverse	TGA TCT GAG TGT GAG GGT CTG G
IL-33 forward	ACT ATG AGT CTC CCT GTC CTG
IL-33 reverse	ACG TCA CCC CTT TGA AGC

Supplemental References

Fontenot, J.D., Gavin, M.A., and Rudensky, A.Y. (2003). Foxp3 programs the development and function of CD4⁺CD25⁺regulatory T cells. *Nature immunology* 4, 330-336.

Li, D., Guabiraba, R., Besnard, A.-G.e., Komai-Koma, M., Jabir, M.S., Zhang, L., Graham, G.J., Kurowska-Stolarska, M., Liew, F.Y., McSharry, C., and Xu, D. (2014). IL-33 promotes ST2-dependent lung fibrosis by the induction of alternatively activated macrophages and innate lymphoid cells in mice. *J Allergy Clin Immunol* 134, 1422-1432.

Stock, A.T., Smith, J.M., and Carbone, F.R. (2014). Type I IFN suppresses Cxcr2 driven neutrophil recruitment into the sensory ganglia during viral infection. *The Journal of experimental medicine* 211, 751-759.